

Published in final edited form as:

J Immunol. 2012 December 15; 189(12): 5809–5819. doi:10.4049/jimmunol.1200889.

Integrins $\alpha\beta3$ and $\alpha4\beta1$ act as co-receptors for fractalkine and the integrin-binding defective mutant of fractalkine is an antagonist of CX3CR1

Masaaki Fujita, Yoko K Takada, and Yoshikazu Takada

Department of Dermatology, and Biochemistry and Molecular Medicine, University of California Davis School of Medicine. Research III Suite 3300, 4645 Second Avenue, Sacramento, CA 95817

Abstract

The membrane-bound chemokine fractalkine (FKN, CX3CL1) on endothelial cells plays a role in leukocyte trafficking. The chemokine domain (FKN-CD) is sufficient for inducing FKN signaling (e.g., integrin activation) and FKN-CD binds to its receptor CX3CR1 on leukocytes. While previous studies suggest that FKN-CD does not directly bind to integrins, our docking simulation studies predicted that FKN-CD directly interacts with integrin $\alpha\beta3$. Consistent with this prediction, we demonstrated that FKN-CD directly bound to $\alpha\beta3$ and $\alpha4\beta1$ at a very high affinity ($K_D = 3.0 \times 10^{-10}$ M to $\alpha\beta3$ in 1 mM Mn^{2+}). Also membrane-bound FKN bound to integrins $\alpha\beta3$ and $\alpha4\beta1$, suggesting that the FKN-CD-integrin interaction is biologically relevant. The binding site for FKN-CD in $\alpha\beta3$ was similar to those for other known $\alpha\beta3$ ligands. wt FKN-CD induced co-precipitation of integrins and CX3CR1 in U937 cells, suggesting that FKN-CD induces ternary complex formation (CX3CR1, FKN-CD, and integrin). Based on the docking model, we generated an integrin-binding defective FKN-CD mutant (the K36E/R37E mutant). K36E/R37E was defective in ternary complex formation and integrin activation, while K36E/R37E still bound to CX3CR1. These results suggest that FKN-CD binding to CX3CR1 is not sufficient for FKN signaling, and that FKN-CD binding to integrins as co-receptors and resulting ternary complex formation is required for FKN signaling. Notably, excess K36E/R37E suppressed integrin activation induced by wt FKN-CD, and effectively suppressed leukocyte infiltration in thioglycollate-induced peritonitis. These findings suggest that K36E/R37E acts as a dominant-negative CX3CR1 antagonist and that FKN-CD/integrin interaction is a novel therapeutic target in inflammatory diseases.

Introduction

The recruitment of leukocytes from the circulation to inflammation sites is a critical event of the inflammatory response regulated by several processes (1, 2): leukocytes capturing and rolling on endothelial cells (Tethering)(3, 4), leukocytes adhesion (Adhesion) (5), and leukocytes transmigration through endothelial layer (Migration). Various adhesion molecules such as selectin, integrins, and chemotactic factors including chemokines are involved in leukocytes trafficking (2, 6–11).

Fractalkine (FKN, CX3CL1) is a chemokine of the CX3C family (12, 13). Unlike most chemokines, FKN is not synthesized by leukocytes, but expressed on the cell surface of

IL-1- and TNF α -activated endothelium as a membrane-bound form (13). FKN is composed of 373 total amino acids consisting of an N-terminal chemokine domain (residues 1–76), a mucin-like stalk (residues 77–317), a transmembrane α helix (residues 318–336), and a short cytoplasmic tail (residues 337–373) (14). Soluble FKN is released by metalloproteinases ADAM10 and ADAM17 (15–17). FKN's highly selective receptor CX3CR1 (a G-protein coupled receptor) is expressed in monocytes, T cell, NK cells, and neuron (18–20). Interaction between membrane-bound FKN and CX3CR1 promotes leukocyte adhesion to endothelium (11, 18, 21).

Integrins are a family of cell adhesion receptors that recognize extracellular matrix ligands and cell surface ligands (22). Activated integrins support both cell migration and adhesion in a cation-dependent manner. Upon activation, integrins undergo a series of conformational changes that result in increased binding affinity for their respective ligands (23). FKN enhances cell adhesion through integrin activation that triggers arrest and firm adhesion. FKN-mediated integrin activation is typically mediated by CX3CR1 engagement (10, 24–27). FKN-CX3CR1 interaction can activate integrin through a mechanism involving G protein-coupled receptors (GPCRs) (21, 28, 29) and enhance cell adhesion to activated endothelial cells (VCAM-1+).

FKN-mediated cell adhesion is robust in the absence of divalent cations, which are required for integrin-mediated adhesion, and neutralizing antibodies against integrins (anti- β 1 and β 2) do not block the FKN-mediated adhesion (18, 21). It has been proposed that FKN-mediated adhesion does not involve the direct binding of integrins to FKN. Thus it has been believed that FKN may mediate cell adhesion and migration directly through binding to CX3CR1 (11, 30) and indirectly through activation of integrins (30–32).

In the present study, we discovered that the chemokine domain of FKN (FKN-CD) binds to integrins α 4 β 1 and α v β 3. The affinity of FKN-CD binding to α v β 3 is extremely high as an integrin ligand ($K_D=3.0 \times 10^{-10}$ M in Mn^{2+}). FKN-CD binds to the ligand-binding site common to other known integrin ligands. The integrin-binding defective FKN-CD mutant (the Lys36 to Glu/Arg37 to Glu (K36E/R37E) mutant) is defective in FKN signaling, while it still binds to CX3CR1. CX3CR1, FKN-CD, and integrin make a ternary complex through the direct integrin binding to FKN-CD. We propose a model in which FKN on endothelial cells binds to leukocytes through CX3CR1 and/or integrins (α v β 3 and α 4 β 1), and in which integrins as well as CX3CR1 are directly involved in FKN signaling and leukocyte trafficking through binding to FKN-CD.

Materials and Methods

Materials

Recombinant soluble α v β 3 was synthesized in Chinese hamster ovary (CHO) K1 cells using the soluble α v and β 3 expression constructs and purified by nickel-nitrilotriacetic acid (Ni-NTA) affinity chromatography as described (33). 7E3 (anti-human integrin β 3) (34) and anti-human β 1 mAb AIIIB2 (35, 36) hybridomas were obtained from ATCC. Anti- α 4 mAb SG73 has been described (37). K562 and U937 cells were obtained from ATCC. K562 erythroleukemia cells that express human α v β 3 (α v β 3-K562) (38) were provided by Eric Brown (University of California, San Francisco). K562 cells that express human α 4, CHO cells that express human β 1, β 3, or β 1–3–1 mutant have been described (39). Cyclic RGDfV was purchased from Enzo Life Sciences (Farmingdale, NY). Rabbit anti-human CX3CR1 was obtained from Torrey Pines Biolab (East Orange, NJ) or from AbD Serotec (Oxford, UK). Mouse anti-human FKN mAb (MAB365) was obtained from R&D systems (Minneapolis, MN). Rabbit anti-human α 4 was obtained from Cell Signaling Technology (Danvers, MA). Anti-human integrin β 3 (I81720) was purchased from BD Biosciences.

Anti-human $\beta 3$ mAb AV10 was kindly provided by B. Felding-Habermann (The Scripps Research Institute, La Jolla, CA).

Synthesis of the chemokine domain of FKN (FKN-CD) and stromal cell-derived factor-1 SDF1

The cDNA fragment of the chemokine domain of FKN was amplified using primers 5'-cgggatcccagcaccacggtgtgacg-3' and 5'-cggattctcagccatttcgagtagggcag with human fractalkine cDNA (Open Biosystems, Lafayette, CO) as a template, and subcloned into the BamHI/EcoRI site of PET28a expression vector. The protein was synthesized in BL21 induced by IPTG as an insoluble protein. The protein was solubilized in 8 M urea, purified by Ni-NTA affinity chromatography and refolded as previously described (40). The amino acid sequence is [MGSSHHHHHSSGLVPRGSHMASMTGGQQMGRGS]QHHGVTKCNITCSKMTSKIP VALLIHYQQNQASC GKRAIILETRQHRLFCADPKEQWVKDAMQHLDRQAAALTRN G. The re-folded protein was >90% homogeneous upon SDS-PAGE.

The cDNA fragment of SDF1 was amplified using primers 5'-cgggatccaagcccgctgacgctgacg-3' and 5'-cggattctcacatcttgacacctgttttaaagc-3' with human SDF1 cDNA (Open Biosystems, Lafayette, CO) as a template, and subcloned into the BamHI/EcoRI site of PET28a expression vector. The protein was synthesized, purified and refolded as described above. The re-folded protein was >90% homogeneous upon SDS-PAGE.

Expression of full-length FKN

The cDNA fragment encoding full-length FKN was amplified using 5'-CCTCGAGGAGCTGTGCCGCCT-3' and 5'-GCTCTAGAGGTGTCTGAATCA-3' as primers with human fractalkine cDNA as a template and subcloned into the XhoI/XbaI site of pBJ-1 expression vector. The full-length FKN expression construct was transfected into CHO cells together with neomycin-resistant plasmid using Fugene (Promega). After selection with G418, cells stably expressing full-length FKN were further enriched by limited dilution to obtain about 50% positive populations.

Cell-cell binding assays

CHO cells that express full-length FKN were plated on wells of 96-well plates (5000 cells/well). K562 or U937 cells were labeled with BCECF-AM and added to the wells (10^5 cells/well). After incubating for 1 h at 37°C, bound K562 or U937 cells were quantified using fluorescent microplate reader (excitation 503 nm, emission 520 nm) after removing unbound cells by gentle rinsing.

Binding of Soluble $\alpha v\beta 3$ to Immobilized FKN-CD

ELISA-type binding assays using soluble $\alpha v\beta 3$ were performed as described previously (40). Briefly, 96-well Immulon-2 microtiter plates (Dynatech Laboratories, Chantilly, VA) were coated with 100 μ l of 0.1 M NaHCO₃ containing fractalkine or its mutants and were incubated for 2 h at 37°C. Remaining protein binding sites were blocked by incubating with PBS/0.1% BSA for 30 min at room temperature. After washing with PBS, soluble recombinant $\alpha v\beta 3$ (5 μ g/ml) in Hepes-Tyroses buffer (10 mM HEPES, 150 mM NaCl, 12 mM NaHCO₃, 0.4 mM NaH₂PO₄, 2.5 mM KCl, 0.1% glucose, 0.1% BSA) with 1 mM MnCl₂ was added to the wells and incubated for 2 h at room temperature. After unbound $\alpha v\beta 3$ were removed by rinsing the wells with binding buffer, bound $\alpha v\beta 3$ was measured using anti-integrin $\beta 3$ (mAb AV-10) followed by horseradish peroxidase-conjugated goat anti-mouse IgG and peroxidase substrates.

Adhesion Assays

Adhesion assays were performed as described previously (40). Briefly, to assess cell adhesion to immobilized FKN-CD, 96-well Immulon-2 microtiter plates were coated with 100 μ l of 0.1 M NaHCO₃ containing FKN-CD or its mutant and were incubated for 2 h at 37°C. Remaining protein binding sites were blocked by incubating with PBS/0.1% BSA for 30 min at room temperature. After washing with PBS, K562 cells, CHO cells, or U937 cells in 100 μ l of RPMI 1640/0.1% BSA or DMEM/0.1% BSA were added to the wells and incubated at 37°C for 1 h. After unbound cells were removed by rinsing the wells with the medium used for adhesion assays, bound cells were quantified by measuring endogenous phosphatase activity (40). To determine cation dependence, HEPES-Tyrodes buffer with 4 mM EDTA, 4 mM CaCl₂, 4 mM MgCl₂, or 4 mM MnCl₂ was used instead of RPMI 1640. To assess the effect of blocking antibodies and cyclic RGDfV, cells were pretreated with mAbs or cRGDfV at room temperature for 30 min before the assay.

Surface Plasmon Resonance Study

Recombinant soluble integrin α v β 3 was immobilized to Biacore Sensor chip CM5 (Biacore, Piscataway, NJ) by the amine coupling method. 2-fold serially diluted FKN-CD or its mutant K36E/R37E in running buffer (HBS-P buffer containing 1 mM MnCl₂, CaCl₂, or MgCl₂) were injected for 3 min at the flow rate of 30 μ l/min. Then the sensor chip was washed with the running buffer alone at the same flow rate for another 15 min (the dissociation phase). 30 seconds injections of regeneration buffer (0.1 M NaOH, 1M NaCl) at the same flow rate were used to regenerate the chip for another cycle of injection. The resonance unit elicited from the reference flow cell was subtracted from the resonance unit elicited from the integrin flow cell to eliminate the nonspecific protein-flow cell interaction and the bulk refractive index effect. The recorded binding curves were analyzed using the BIAevaluation Version 4.

Chemotaxis

Chemotaxis was measured in modified Boyden chambers (Transwells). wt FKN-CD, K36E/R37E, or R47A (1 and 10 ng/ml, total 600 μ l RPMI 1640 medium) was placed in the lower chamber, and U937 cells (5×10^5 cells per well) were placed in the upper chamber. After 4 h incubation at 37°C, cells in the lower chamber was counted.

Pull-down assays

We incubated the wt and mutant FKN-CD (1 or 10 μ g/ml, with 6His tag) with lysates of U937 cells and recovered FKN-CD with Ni-NTA-Sepharose, and analyzed the bound CX3CR1 by western blotting.

Co-precipitation of integrins, CX3CR1, and FKN-CD

U937 cells were cultured to nearly confluent in RPMI 1640/10% FCS. The cells were resuspended with RPMI 1640 and incubated with 1 μ g/ml wt or K36E/R37E for 15 min. The cells were lysed with lysis buffer (20 mM HEPES (pH 7.4), 100 mM NaCl, 10% glycerol, 1% NP-40, 1 mM MgCl₂, 1 mM PMSF, protease inhibitors cocktail (Sigma-Aldrich)). Cell lysate were incubated with anti-integrin β 3 antibody or anti-integrin α 4 antibody overnight at 4°C, and the immune complex was recovered by incubating with protein A Sepharose (GE Healthcare) for 1 h at 4°C and washed three times with wash buffer (20 mM HEPES (pH 7.4), 100 mM NaCl, 10% glycerol, 0.5% NP-40, 1 mM MgCl₂, 1 mM PMSF, protease inhibitors cocktail). The immunoprecipitated materials were analyzed by Western Blotting with anti-CX3CR1 antibody.

Flow cytometry

U937 cells were cultured to nearly confluent in RPMI 1640/10% FCS. The cells were resuspended with RPMI 1640/0.1% BSA and incubated for 30 min at room temperature to block remaining protein binding sites. And the cells were incubated with wt FKN-CD (or SDF1) and/or K36E/R37E for 5 min at room temperature and then incubated with FITC-labeled ligands (Fibrinogen γ C399tr, Fibronectin-8-11, or Fibronectin-H120) for 15 min at room temperature. For blocking experiments, the cells were pre-incubated with antibodies (KH72, SG73, AIIB2, or 7E3) for 30 min at room temperature before incubation with FKN. The cells were washed with PBS/0.02% BSA and analyzed by FACSCalibur (Becton Dickinson, MountainView, CA).

Thioglycollate-induced peritonitis

We injected wt FKN-CD and/or K36E/R37E in PBS i.p. to mice and 3 h later injected 1 ml 3% thioglycollate. Mice were killed 48 h after thioglycollate injection, and peritoneal exudate cells were harvested by peritoneal lavage using ice-cold RPMI1640/10%FBS. Cells were counted on a hemocytometer and then differential cell counts were conducted after staining with Hem-3 (Fischer). Data are shown as means \pm S.E., and statistical analysis was performed using one-way ANOVA and Tukey post-hoc analysis.

In vitro stability of FKN-CD

6His-tagged wt FKN-CD (1 μ g) was added to whole mouse serum (20 μ l) and incubated for 15 to 60 min and analyzed by western blotting using anti-6His antibody. In another experiment, 6His-tagged wt FKNCD (1 μ g) was incubated with U937 cells (1×10^5 cells per sample) in RPMI 1640 medium in the presence or absence of FCS (10%) for 5 to 60 min. Bound wt FKN-CD was detected using Alexa488-anti-6His antibody and flow cytometry.

Co-precipitation of membrane-bound FKN and integrin β 3 or α 4

Cell lysates of FKN-CHO cells and U937 cells were mixed and incubated for 1 h at 4°C, and then the mixture was incubated with anti- β 3 or anti- α 4 mAb for additional 1 h at 4°C. The immune complex was recovered by incubating with protein A-Sepharose for 30 min at 4°C, and analyzed by western blotting with anti-CX3CR1 antibody.

Other methods

Docking simulation of interaction between FKN-CD and integrin α v β 3 was performed using AutoDock3 as described (41). Treatment differences were tested using ANOVA and Tukey's multiple comparison test to control the global type I error using Prism 5.0a (Graphpad Software).

Results

FKN-CD binds to integrin α v β 3

The chemokine domain of FKN (FKN-CD) is sufficient for FKN binding to cells (42, 43). We performed docking simulation of the interaction between integrin α v β 3 (PDB code 1L5G) and FKN-CD (PDB code 1F2L) using AutoDock3. The simulation predicted that FKN-CD binds to α v β 3 at a high affinity (docking energy -24.7 Kcal/mol) (Fig. 1a). The prediction is not consistent with previous reports. It has been believed that FKN-mediated adhesion is independent of integrins (18). We thus studied whether FKN-CD directly binds to integrin α v β 3. We found that recombinant soluble α v β 3 bound to immobilized FKN-CD in a dose-dependent manner in ELISA-type binding assays (Fig. 1b). Heat-denaturation markedly reduced α v β 3 binding to FKN-CD, suggesting that proper folding of the protein is required for integrin binding. K562 erythroleukemic cells do not express CX3CR1 (21). We

found that K562 cells ($\alpha 5\beta 1+$) that express exogenous $\alpha v\beta 3$ ($\alpha v\beta 3$ -K562, $\alpha 5\beta 1+/\alpha v\beta 3+$) strongly adhered to FKN-CD, but mock-transfected K562 cells showed only weak adhesion to FKN-CD (Fig. 1c). The adhesion of $\alpha v\beta 3$ -K562 cells to FKN-CD showed cation dependency and there are significant adhesion of $\alpha v\beta 3$ -K562 to FKN-CD in the presence of Ca^{2+} and EDTA: $\text{Mn}^{2+} > \text{Mg}^{2+} = \text{Ca}^{2+} = \text{EDTA}$ (Fig. 1d). To assess the affinity of FKN-CD to bind to $\alpha v\beta 3$, we performed surface plasmon resonance (SPR) studies using a sensor chip immobilized with soluble $\alpha v\beta 3$ (Fig. 1e). FKN-CD bound to $\alpha v\beta 3$ at a very high affinity: $K_D = 1.1 \times 10^{-8}$ M in 1 mM Ca^{2+} (Fig. 1e), $K_D = 6.9 \times 10^{-9}$ M in 1 mM Mg^{2+} and $K_D = 3.0 \times 10^{-10}$ M in 1 mM Mn^{2+} (data not shown) in contrast to previous reports. However, mAb 7E3 (anti- $\beta 3$ blocking antibody) and cyclic RGDfV, an antagonist specific to $\alpha v\beta 3$ (44), did not effectively block the adhesion of $\alpha v\beta 3$ -K562 cells to FKN-CD (data not shown).

The specificity loop of $\beta 3$ plays a role in recognition of FKN-CD

To determine if FKN-CD is a ligand for integrin $\alpha v\beta 3$, we identified amino acid residues in $\beta 3$ that are critical for FKN-CD binding. We previously showed that when a disulfide-linked loop of $\beta 1$ I-like domain (residues 187–193) is swapped with a corresponding sequence in $\beta 3$ integrin (designated the $\beta 1$ -3-1 mutant) (Fig. 2a), ligand-binding specificity of the mutated integrin $\alpha v\beta 1$ -3-1 is altered to that of $\alpha v\beta 3$ (45). Hence the loop was designated “the specificity loop”. Consistent with the idea that the specificity loop determines ligand specificity, the loop is in the ligand-binding sites in the $\alpha v\beta 3$ crystal structure and exposed to the surface (46). The specificity loop is diverse in sequence, and present in all β subunits except for $\beta 4$, in which the loop is deleted and replaced with two remnant residues. The $\beta 1$ -3-1 mutant binds to several $\alpha v\beta 3$ ligands (40, 41, 45, 47–49), which do not bind to wt $\beta 1$ integrins in CHO cells. We tested if the specificity loop of $\beta 3$ is involved in FKN-CD binding to $\alpha v\beta 3$. We found that CHO cells that express $\beta 1$ -3-1 ($\beta 1$ -3-1-CHO cells) adhered to FKN-CD at the level comparable to that of CHO cells that express $\beta 3$ (Fig. 2b). It has been reported that CHO cells do not express CX3CR1 (50). We demonstrated that anti-human $\beta 1$ mAb AIIB2 significantly reduced adhesion of $\beta 1$ -3-1-CHO cells to FKN-CD (Fig. 2c) (Note that $\beta 1$ -3-1 is $>99\%$ $\beta 1$), suggesting that the binding is specific. These findings suggest that the FKN-CD binding site in $\beta 3$ overlaps with those of other known $\alpha v\beta 3$ ligands.

Amino acid residues in FKN-CD that are involved in integrin binding

To identify the integrin-binding site in FKN-CD, we introduced mutations within the integrin-binding site of FKN-CD, which has been predicted by docking simulation (Table 1). We selected Lys36, Arg37, Lys54, and Lys59 of FKN-CD for mutagenesis and mutated them individually or in combination to Glu or Ala. We found that the Lys36/Arg37 to Glu (K36E/R37E) mutation and to a less extent the Lys36/Arg37 to Ala (K36A/R37A) mutation, reduced the binding of soluble $\alpha v\beta 3$ to FKN-CD in ELISA-type binding assays, while the Lys54 to Ala (K54A) or Lys54/Lys59 to Ala (K54A/K59A) mutation had little or no effect on integrin binding (Figs. 3a and 3b). As a control, we mutated Arg47, which is involved in CX3CR1 binding (42, 43), to Ala (R47A). The R47A mutation had little or no effect on integrin binding (Figs. 3a–d). In adhesion assays, the K36E/R37E mutant was defective in supporting adhesion of $\alpha v\beta 3$ -K562 cells as well (Fig. 3c). K562 cells that express endogenous integrin $\alpha 5\beta 1$ weakly adhered to wt FKN (Figs. 1c and 3d), suggesting that $\alpha 5\beta 1$ weakly binds to FKN-CD. In SPR studies, the K36E/R37E mutant bound to $\alpha v\beta 3$ at an affinity much lower (>100 times) than that of wt FKN-CD ($K_D = 2.7 \times 10^{-6}$ M in 1 mM Ca^{2+} , 4.3×10^{-7} M in 1 mM Mg^{2+} , and 2.0×10^{-8} M in 1 mM Mn^{2+}). Taken together, these findings suggest that the K36E/R37E mutation of FKN-CD effectively suppresses integrin binding and that the integrin- and the CX3CR1-binding sites of FKN-CD are distinct.

We tested if the K36E/R37E mutation affects the binding of FKN-CD to CX3CR1 by pull-down assays. We incubated the wt and K36E/R37E FKN-CD (with 6His tag) with lysates of U937 cells and recovered FKN-CD with Ni-NTA-Sepharose, and analyzed the bound CX3CR1 by western blotting. wt FKN-CD and K36E/R37E bound to CX3CR1 while R47A (a negative control) was defective in this function, suggesting that the K36E/R37E mutation does not affect the binding to CX3CR1 (Fig. 3e).

FKN-CD binds to $\alpha 4\beta 1$ and the K36E/R37E mutation reduces the interaction

We have shown so far that FKN-CD binds to $\alpha v\beta 3$, but it is not a major integrin in leukocytes. We tested the possibility that $\alpha 4\beta 1$, a major integrin in immune-competent cells, interacts with FKN-CD. K562 cells ($\alpha 5\beta 1+$) expressing exogenous $\alpha 4\beta 1$ ($\alpha 4$ -K562, $\alpha 5\beta 1+\alpha 4\beta 1+$) adhered to FKN-CD (Fig. 4a) stronger than mock-transfected K562 cells (Fig. 3d). The K36E/R37E mutant was defective in binding to $\alpha 4\beta 1$, suggesting that $\alpha 4\beta 1$ -binding site in FKN-CD is similar to that of $\alpha v\beta 3$. Anti- $\alpha 4$ mAb SG73 and anti- $\beta 1$ mAb AIIB2 suppressed FKN-CD binding to $\alpha 4$ -K562 cells in adhesion assays (Fig. 4b). When $\alpha 4$ -K562 cells were incubated with FITC-labeled soluble FKN-CD, mAb AIIB2 and SG73 suppressed the binding of FKN-CD (data not shown). These findings suggest that $\alpha 4\beta 1$ specifically binds to FKN-CD. The $\alpha 4\beta 1$ -FKN-CD interaction was cation-dependent: $\alpha 4$ -K562 adhesion to FKN-CD is the strongest in Mn^{2+} , and was not completely suppressed by Ca^{2+} or EDTA (Fig. 4c).

Relative contribution of CX3CR1 and integrins to adhesion of U937 cells (CX3CR1+) to FKN-CD

We demonstrated so far that FKN-CD supports cell adhesion through integrin binding in cells that do not express CX3CR1 (K562 and CHO cells). It has been reported that FKN-CD binding to its specific receptor CX3CR1 plays a role in leukocyte adhesion and migration (18, 21). We thus determined the relative contribution of CX3CR1 and integrins to the binding of U937 cells (which express CX3CR1) to FKN-CD. U937 cells efficiently adhered to wt FKN-CD in a dose dependent manner (Fig. 5a), while U937 cells adhered to K36E/R37E or R47A less efficiently (about 40–45%). This is in contrast to $\alpha v\beta 3$ - or $\alpha 4$ -K562 cells (which do not express CX3CR1): both cell lines bound to both wt FKN-CD and R47A equally well, and much less efficiently to K36E/R37E (Fig. 3). These results suggest that both CX3CR1 and integrins play a role in the binding of FKN-CD to U937 cells that express both CX3CR1 and integrins ($\alpha 4\beta 1$ and $\alpha v\beta 3$). The binding of FKN-CD to U937 cells showed cation dependency that is similar to those of $\alpha v\beta 3$ and $\alpha 4\beta 1$ binding (Fig. 5b). We found that mAb SG73 (anti- $\alpha 4$) and AIIB2 (anti- $\beta 1$) effectively suppressed the binding of FKN-CD to U937 cells (Figs. 5c and 5d). These results suggest that $\alpha 4\beta 1$ is involved in FKN-CD binding to U937 cells. We could not determine the contribution of other integrins (e.g., $\alpha v\beta 3$ and $\alpha 5\beta 1$) to FKN-CD binding to U937 cells because antagonists to $\alpha v\beta 3$ (mAb 7E3 or cRGDfV) or that of $\alpha 5\beta 1$ (mAb KH72) did not affect the binding of U937 cells to FKN-CD (data not shown).

We tested if the K36E/R37E mutation affects the ability of FKN-CD to induce chemotaxis. We found that both wt FKN-CD and K36E/R37E induced chemotaxis of U937 cells, while the R47A mutant was very defective in this function (Fig. 5e). These results suggest that chemotaxis is CX3CR1-dependent but not integrin-dependent.

FKN-CD induces co-precipitation of integrin $\alpha 4$ and $\beta 3$ and CX3CR1 in U937 cells and the co-precipitation requires direct integrin binding to FKN

We tested the hypothesis that integrin and CX3CR1 can bind simultaneously to FKN-CD by co-immunoprecipitation. We stimulated U937 cells with wt or mutant FKN-CD and immuno-purified integrin $\alpha 4$ or $\beta 3$ from cell lysates, and analyzed the purified materials by

western blotting. We detected CX3CR1 in the purified materials from cells stimulated by wt FKN-CD, but not those from cells that was not stimulated or those from cells stimulated by K36E/R37E or R47A (Figs. 5f and 5g). These results suggest that FKN-CD, CX3CR1, and integrins ($\alpha 4\beta 1$ or $\alpha v\beta 3$) make a ternary complex upon FKN-CD stimulation, and that the ternary complex formation requires simultaneous binding of CX3CR1 and integrins to FKN-CD.

K36E/R37E suppresses integrin activation induced by FKN-CD (a dominant-negative effect)

If direct integrin binding to FKN-CD and subsequent ternary complex formation is involved in FKN signaling, it is predicted that the integrin-binding defective FKN-CD mutant (K36E/R37E) suppresses signals induced by wt FKN-CD. It has been reported that FKN binding to CX3CR1 enhances cell adhesion by activating integrin through inside-out signaling (30–32). We tested if K36E/R37E suppresses integrin activation that is induced by wt FKN-CD. We used integrin ligands that are specific to $\alpha 5\beta 1$ (fibronectin type III domains 8–11, FN 8–11) (51, 52), $\alpha 4\beta 1$ (fibronectin H120 fragment, FN H120) (53) and $\alpha v\beta 3$ (fibrinogen γ -chain C-terminal domain that lacks residues 400–411 (γ C399tr)) (48). We measured the binding of soluble labeled ligands to U937 cells in flow cytometry. wt FKN-CD enhanced ligand binding to these integrins in a dose-dependent manner, while K36E/R37E was defective in this function (Fig. 6a–d). Notably excess K36E/R37E suppressed the ligand binding to the integrins induced by wt FKN-CD in a dose-dependent manner (Fig. 6a–c, 6e and 6f). These findings suggest that K36E/R37E is a dominant-negative antagonist to CX3CR1.

We next tested if the inhibitory effect of K36E/R37E on integrin activation is receptor-specific. Stromal cell-derived factor-1 (SDF1, CXCL12), a member of the CXC chemokine family, activates integrin $\alpha 4\beta 1$ in a CXCR4-dependent manner (54–56). We found that K36E/R37E did not affect SDF1-induced binding of FN-H120 to integrin $\alpha 4\beta 1$ in U937 cells (Fig. 6g). This suggests that the inhibition of $\alpha 4\beta 1$ activation by K36E/R37E is specific to CX3CR1, and does not affect CXCR4-mediated integrin activation.

K36E/R37E suppresses leukocyte infiltration in thioglycollate-induced peritonitis

The *in vivo* inhibitory action of K36E/R37E was evaluated further in a noninfectious peritonitis model (57). We injected K36E/R37E to mice and 3 h later injected thioglycollate. Forty-eight h after thioglycollate injection, peritoneal exudate cells were harvested by peritoneal lavage. Thioglycollate treatment markedly enhanced total leukocyte cell number (Fig. 7a). About 70% of total leukocytes 48 h after thioglycollate injection was monocytes/macrophage (Fig. 7b) and 10–20% neutrophils, consistent with a previous report (57). K36E/R37E strongly inhibited the thioglycollate-induced accumulation of leukocytes and wt FKN-CD enhanced it. In mice treated with WT FKN and excess K36E/R37E (20 \times) the total and monocyte/macrophage levels were below those of thioglycollate only (Fig. 7a and b), suggesting that excess K36E/R37E suppresses leukocyte recruitment induced by exogenous and endogenous FKN. The effect of wt FKN-CD and/or K36E/R37E to neutrophils was similar to that of monocytes/macrophages but was not conclusive probably because neutrophils levels were already off the peak and the number of neutrophils are low 48 h after thioglycollate injection (data not shown). These results suggest that K36E/R37E can induce the dominant-negative effect in *in vivo* model of inflammation and neutralize endogenous and exogenous FKN. Interestingly, WT FKN-CD (without thioglycollate) significantly enhanced the total and monocytes/macrophages, confirming that FKN-CD is able to recruit leukocytes by itself. These data demonstrate K36E/R37E suppresses the recruitment of inflammatory cells in a mouse model of inflammation.

Is FKN-CD present in circulation after 48 h? To address this question, we tested if the serum samples of mice that have been injected with wt FKN-CD or K36E/R37E (6His-tagged) still contain 6His-tagged proteins by western blotting. We did not detect any signals (data not shown). We studied the in vitro stability of FKN-CD by incubating FKN-CD with medium with or without serum (FCS or mouse serum). We found that FKN-CD was quickly degraded in these conditions (half-life about 30 min) (Supplemental Fig. S1). So it is highly likely that wt FKN-CD and K36E/R37E trigger their signals and rapidly disappear from circulation in vivo.

Do integrins interact with membrane-bound FKN?

Our results so far suggest that the isolated FKN-CD interacts with integrins. We studied if integrins interact with the membrane-bound FKN since FKN is usually expressed in a membrane-bound form on the cell surface. We stably expressed wt full-length FKN in CHO cells (designated FKN-CHO cells). We found that $\alpha v\beta 3$ -K562, $\alpha 4$ -K562, and U937 cells bound to FKN-CHO cells better than to mock-transfected CHO cells in cell-cell binding assays (Fig. S2). Control K562 cells only weakly bound to FKN-CHO cells. This suggests that integrins bind to membrane-bound FKN on the cell surface. We found that membrane-bound FKN induced ternary complex formation with CX3CR1 and integrins $\alpha v\beta 3/\alpha 4\beta 1$ (Fig. S2). This indicates that the chemokine domain of natural membrane-bound FKN can simultaneously interact with integrins and CX3CR1.

Taken together, the present study suggests that FKN-CD is a ligand for $\alpha v\beta 3$ and $\alpha 4\beta 1$, in contrast to previous studies, and the direct integrin binding of FKN-CD or full-length FKN is involved in FKN signaling. An integrin-binding defective mutant is defective in FKN signaling, while it still binds to CX3CR1, and is a dominant-negative mutant.

Discussion

In the present study, we first predicted that FKN-CD may bind to integrin $\alpha v\beta 3$ at a high affinity using docking simulation. We then demonstrated that FKN-CD binds to integrins and supports cell adhesion in a CX3CR1-independent manner, since FKN-CD bound to recombinant soluble $\alpha v\beta 3$ and supported adhesion of $\alpha v\beta 3$ -K562 cells that do not express CX3CR1. We found that mutating two amino acid residues (Lys36 and Arg37) in FKN-CD in the predicted integrin-binding site (the K36E/R37E mutation) suppressed binding to $\alpha v\beta 3$. The K36E/R37E mutant still bound to CX3CR1, suggesting that integrin-binding site and CX3CR1-binding site in FKN-CD are distinct. The FKN-CD binding site in $\alpha v\beta 3$ overlaps with those of other known $\alpha v\beta 3$ ligands since the specificity loop of $\beta 3$ is involved in recognition of FKN-CD. Furthermore, SPR studies suggest that FKN-CD binds to $\alpha v\beta 3$ at an extremely high affinity, and the K36E/R37E mutation markedly reduces the binding function of FKN-CD to $\alpha v\beta 3$. These findings establish that FKN-CD is a high-affinity ligand for $\alpha v\beta 3$.

However, mAb 7E3 specific to integrin $\beta 3$ or a small molecule inhibitor cyclic RGDfV did not suppress the binding of FKN-CD to $\alpha v\beta 3$. mAb 7E3 has been mapped within the ligand binding site of $\beta 3$ (58, 59) and K_D to $\alpha v\beta 3$ is 2.5×10^{-9} M (34). One possibility is that 7E3 did not suppress FKN-CD binding to $\alpha v\beta 3$ because FKN-CD has a high binding affinity to $\alpha v\beta 3$. Another possibility is that the binding site for FKN-CD is not exactly the same as those of other known $\alpha v\beta 3$ ligands, and therefore 7E3 did not block the access of FKN-CD to $\alpha v\beta 3$. Cyclic RGDfV has K_D 2.4×10^{-9} M to $\alpha v\beta 3$ (60). It is again possible that the affinity of cyclic RGDfV may not be high enough to effectively suppress FKN-CD. Another possibility is that the RGD-binding site was not critically involved in FKN-CD binding, and therefore cyclic RGDfV did not induce steric hindrance to FKN-CD in $\alpha v\beta 3$. Consistent with this idea, anti- $\beta 1$ mAb AIIB2, which affects conformation of $\beta 1$ rather than blocking

access of ligands to the binding site (36), did suppress the binding of $\beta 1$ -3-1-CHO cells to FKN-CD.

We also demonstrated that FKN-CD bound to another integrin $\alpha 4\beta 1$. In this case, function-blocking anti- $\alpha 4$ mAb SG73, which is mapped within the ligand-binding site of $\alpha 4$ (37), and anti- $\beta 1$ mAb AIIB2 suppressed this interaction in $\alpha 4$ -K562 and U937 cells. Since $\alpha 4\beta 1$ is expressed in leukocytes, $\alpha 4\beta 1$ -FKN-CD interaction is expected to contribute to FKN binding to leukocytes during trafficking of leukocytes. Since the K36E/R37E mutant was defective in $\alpha 4\beta 1$ binding, it is suggested that $\alpha 4\beta 1$ binds to FKN-CD in a manner similar to that of $\alpha v\beta 3$. Since $\alpha 4\beta 1$ is a major FKN-CD binding integrin in U937 cells, it is likely that $\alpha 4\beta 1$ is important in FKN signaling in macrophages/monocytes, T-cells, and NK cells, in which both CX3CR1 and $\alpha 4\beta 1$ are expressed.

We demonstrated that FKN-CD binds to $\alpha v\beta 3$ - or $\alpha 4$ -K562 cells through $\alpha v\beta 3$ or $\alpha 4\beta 1$ and to a much less extent, through $\alpha 5\beta 1$ in a CX3CR1-independent manner. In the case of U937 cells that express both CX3CR1 and integrins ($\alpha 4\beta 1$ + and $\alpha v\beta 3$ weakly +), we demonstrated that FKN-CD binds to cells in an integrin-dependent and/or CX3CR1-dependent manner.

Importantly, we obtained similar results in integrin binding using the membrane-bound FKN. This suggests that 1) integrins can access to the chemokine domain in the membrane-bound FKN, and 2) integrins, membrane-bound FKN, and CX3CR1 can make a ternary complex. We did not, however, show if integrins access to FKN in cis and/or in trans in the present study.

Why direct integrin binding to the chemokine domain of FKN was overlooked? It has been proposed that FKN binding to CX3CR1-transfected K562 cells is integrin-independent, since EDTA does not block the binding (18). In the present study, we demonstrated that EDTA did not fully suppress FKN-CD binding to integrins $\alpha v\beta 3$ and $\alpha 4\beta 1$. Also, previous studies used the chemokine domain (76 amino acid residues) fused with large secretory placenta alkaline phosphatase (484 amino acid residues) (CX3CL1-SEAP) (21, 32). It has been reported that macrophage-like cell line THP-1 cells efficiently adhered to immobilized CX3CL1-SEAP and anti- $\beta 1$ antibodies did not suppress the adhesion (21). It has also been reported that THP-1 cells effectively bind to TNF α -stimulated human umbilical vein endothelial cells (HUVEC) and anti- $\beta 1$ and $\beta 2$ antibodies partially suppressed the binding (21). Since TNF α -stimulated endothelial cells express VCAM-1, ICAM-1, and FKN, it is unclear if the antibodies suppressed integrin binding to VCAM-1, ICAM-1, or FKN. The present study identified that anti- $\beta 1$ AIIB2 and anti- $\alpha 4$ SG73 suppress integrin-FKN-CD interaction, but did not determine which of other anti-integrin antibodies effectively suppress integrin binding to FKN-CD at this point. It is possible that the mAbs used (anti- $\beta 1$) in previous studies did not effectively block the access of FKN to integrins because FKN-CD is smaller than other ligands (e.g., fibronectin) or because the affinity of the antibodies to $\beta 1$ integrins is lower than that of FKN-CD. We also suspect that CX3CL1-SEAP is defective in integrin binding possibly due to steric hindrance. One possible reason why we detected integrin-FKN-CD interaction in the present study may be that we used the chemokine domain with a relatively small tag (34 amino acid residues). FKN is expressed as the membrane-bound form. Importantly, we found that membrane-bound FKN induced ternary complex formation with CX3CR1 and integrins $\alpha v\beta 3/\alpha 4\beta 1$ (Fig. S2). This indicates that the chemokine domain of natural membrane-bound FKN can simultaneously interact with integrins and CX3CR1. Thus FKN-integrin interaction is biologically relevant.

In a current model of the FKN-mediated leukocyte trafficking, FKN captures leukocytes in a selectin- and integrin-independent manner (14). Interaction between FKN and CX3CR1 can

also activate integrins, resulting in firmer adhesion. Leukocytes then extravasate through the vascular wall and into the tissue to a chemokine gradient. FKN may facilitate extravasation of circulating leukocytes by mediating cell adhesion through the initial tethering and final transmigration steps (14). In this model integrins are involved only in the firm adhesion step. The present study suggests that FKN-integrin interaction may be involved a) in the initial capturing of leukocytes through direct binding to FKN, and b) in the activation of integrins through CX3CR1 as well. Interestingly, K36E/R37E induced chemotaxis at the level comparative to that of wt FKN-CD, while R47A did not. This suggests that FKN-induced chemotaxis is CX3CR1-dependent and FKN-CD-integrin interaction may not be involved in chemotaxis.

What is the role of integrins in FKN signaling? In U937 cells (CX3CR1+), we demonstrated that integrins ($\alpha\text{v}\beta\text{3}$ and $\alpha\text{4}\beta\text{1}$), FKN-CD, and CX3CR1 generated a ternary complex, while the K36E/R37E mutant was defective in ternary complex formation, suggesting that the direct integrin-FKN interaction plays a critical role in the ternary complex formation. Based on these findings we propose a novel model of FKN signaling, in which FKN binding to CX3CR1 recruits integrins to the complex, resulting in the formation of a ternary complex (CX3CR1-FKN-integrin) on the cell surface. If the ternary complex formation is required for proper FKN signaling, it is predicted that the FKN-CD mutant that is defective in integrin binding will exert as an antagonist of this signaling pathway. Consistent with the prediction, we demonstrated that excess K36E/R37E suppressed integrin activation in vitro, and leukocyte infiltration in thioglycollate-induced peritonitis in vivo. Also, K36E/R37E suppressed the increase in leukocyte recruitment induced by wt FKN-CD. These findings suggest that the K36E/R37E mutant acts as a dominant-negative antagonist of FKN signaling and neutralize endogenous and exogenous FKN. The K36E/R37E mutant may have potential as a therapeutic agent in inflammatory diseases. Collagen-induced rheumatoid arthritis and experimental autoimmune myositis are disease models with well-defined FKN contribution in which anti-FKN antibodies suppress inflammation (61,62). In future studies we will evaluate the potential of K36E/R37E to suppress chronic inflammation and compare the efficacy of K36E/R37E with that of anti-FKN antibodies in these disease models. It would also be imperative to study molecular mechanisms of integrin contribution in FKN signaling in future studies.

Supplementary Material

Refer to Web version on PubMed Central for supplementary material.

Acknowledgments

We thank E. Brown and B. Felding-Habermann for reagents and Lan Yu for help in peritonitis assays.

This work was supported by TRDRP (Tobacco-related disease research program) 18XT-0169, NIH CA13015, and DOD W81XWH-10-1-0312 (to YT).

References

1. Springer TA. Traffic signals for lymphocyte recirculation and leukocyte emigration: the multistep paradigm. *Cell*. 1994; 76:301–314. [PubMed: 7507411]
2. Lloyd AR, Oppenheim JJ, Kelvin DJ, Taub DD. Chemokines regulate T cell adherence to recombinant adhesion molecules and extracellular matrix proteins. *J Immunol*. 1996; 156:932–938. [PubMed: 8558019]
3. Ley K, Tedder TF. Leukocyte interactions with vascular endothelium. New insights into selectin-mediated attachment and rolling. *J Immunol*. 1995; 155:525–528. [PubMed: 7541818]

4. Tedder TF, Steeber DA, Chen A, Engel P. The selectins: vascular adhesion molecules. *FASEB J*. 1995; 9:866–873. [PubMed: 7542213]
5. Bargatze RF, Butcher EC. Rapid G protein-regulated activation event involved in lymphocyte binding to high endothelial venules. *J Exp Med*. 1993; 178:367–372. [PubMed: 8315393]
6. Charo IF, Ransohoff RM. The many roles of chemokines and chemokine receptors in inflammation. *N Engl J Med*. 2006; 354:610–621. [PubMed: 16467548]
7. Tanaka Y, Adams DH, Hubscher S, Hirano H, Siebenlist U, Shaw S. T-cell adhesion induced by proteoglycan-immobilized cytokine MIP-1 β . *Nature*. 1993; 361:79–82. [PubMed: 7678446]
8. Taub DD, Conlon K, Lloyd AR, Oppenheim JJ, Kelvin DJ. Preferential migration of activated CD4+ and CD8+ T cells in response to MIP-1 α and MIP-1 β . *Science*. 1993; 260:355–358. [PubMed: 7682337]
9. Taub DD, Lloyd AR, Conlon K, Wang JM, Ortaldo JR, Harada A, Matsushima K, Kelvin DJ, Oppenheim JJ. Recombinant human interferon-inducible protein 10 is a chemoattractant for human monocytes and T lymphocytes and promotes T cell adhesion to endothelial cells. *J Exp Med*. 1993; 177:1809–1814. [PubMed: 8496693]
10. Campbell JJ, Hedrick J, Zlotnik A, Siani MA, Thompson DA, Butcher EC. Chemokines and the arrest of lymphocytes rolling under flow conditions. *Science*. 1998; 279:381–384. [PubMed: 9430588]
11. Fong AM, Robinson LA, Steeber DA, Tedder TF, Yoshie O, Imai T, Patel DD. Fractalkine and CX3CR1 mediate a novel mechanism of leukocyte capture, firm adhesion, and activation under physiologic flow. *J Exp Med*. 1998; 188:1413–1419. [PubMed: 9782118]
12. Pan Y, Lloyd C, Zhou H, Dolich S, Deeds J, Gonzalo JA, Vath J, Gosselin M, Ma J, Dussault B, Woolf E, Alperin G, Culpepper J, Gutierrez-Ramos JC, Gearing D. Neurotactin, a membrane-anchored chemokine upregulated in brain inflammation. *Nature*. 1997; 387:611–617. [PubMed: 9177350]
13. Bazan JF, Bacon KB, Hardiman G, Wang W, Soo K, Rossi D, Greaves DR, Zlotnik A, Schall TJ. A new class of membrane-bound chemokine with a CX3C motif. *Nature*. 1997; 385:640–644. [PubMed: 9024663]
14. Umehara H, Bloom ET, Okazaki T, Nagano Y, Yoshie O, Imai T. Fractalkine in vascular biology: from basic research to clinical disease. *Arterioscler Thromb Vasc Biol*. 2004; 24:34–40. [PubMed: 12969992]
15. Garton KJ, Gough PJ, Blobel CP, Murphy G, Greaves DR, Dempsey PJ, Raines EW. Tumor necrosis factor- α -converting enzyme (ADAM17) mediates the cleavage and shedding of fractalkine (CX3CL1). *J Biol Chem*. 2001; 276:37993–38001. [PubMed: 11495925]
16. Chapman GA, Moores K, Harrison D, Campbell CA, Stewart BR, Strijbos PJ. Fractalkine cleavage from neuronal membranes represents an acute event in the inflammatory response to excitotoxic brain damage. *J Neurosci*. 2000; 20:RC87. [PubMed: 10899174]
17. Hundhausen C, Misztela D, Berkhout TA, Broadway N, Saftig P, Reiss K, Hartmann D, Fahrenholz F, Postina R, Matthews V, Kallen KJ, Rose-John S, Ludwig A. The disintegrin-like metalloproteinase ADAM10 is involved in constitutive cleavage of CX3CL1 (fractalkine) and regulates CX3CL1-mediated cell-cell adhesion. *Blood*. 2003; 102:1186–1195. [PubMed: 12714508]
18. Imai T, Hieshima K, Haskell C, Baba M, Nagira M, Nishimura M, Kakizaki M, Takagi S, Nomiyama H, Schall TJ, Yoshie O. Identification and molecular characterization of fractalkine receptor CX3CR1, which mediates both leukocyte migration and adhesion. *Cell*. 1997; 91:521–530. [PubMed: 9390561]
19. Lucas AD, Bursill C, Guzik TJ, Sadowski J, Channon KM, Greaves DR. Smooth muscle cells in human atherosclerotic plaques express the fractalkine receptor CX3CR1 and undergo chemotaxis to the CX3C chemokine fractalkine (CX3CL1). *Circulation*. 2003; 108:2498–2504. [PubMed: 14581400]
20. Schafer A, Schulz C, Eigenthaler M, Fraccarollo D, Kobsar A, Gawaz M, Ertl G, Walter U, Bauersachs J. Novel role of the membrane-bound chemokine fractalkine in platelet activation and adhesion. *Blood*. 2004; 103:407–412. [PubMed: 12969973]

21. Goda S, Imai T, Yoshie O, Yoneda O, Inoue H, Nagano Y, Okazaki T, Imai H, Bloom ET, Domae N, Umehara H. CX3C-chemokine, fractalkine-enhanced adhesion of THP-1 cells to endothelial cells through integrin-dependent and -independent mechanisms. *J Immunol.* 2000; 164:4313–4320. [PubMed: 10754331]
22. Hynes RO. Integrins: bidirectional, allosteric signaling machines. *Cell.* 2002; 110:673–687. [PubMed: 12297042]
23. Luo BH, Carman CV, Springer TA. Structural Basis of Integrin Regulation and Signaling. *Annu Rev Immunol.* 2007; 25:619–647. [PubMed: 17201681]
24. Weber C. Novel mechanistic concepts for the control of leukocyte transmigration: specialization of integrins, chemokines, and junctional molecules. *J Mol Med (Berl).* 2003; 81:4–19. [PubMed: 12545245]
25. Smith ML, Olson TS, Ley K. CXCR2- and E-selectin-induced neutrophil arrest during inflammation in vivo. *J Exp Med.* 2004; 200:935–939. [PubMed: 15466624]
26. Smith DF, Galkina E, Ley K, Huo Y. GRO family chemokines are specialized for monocyte arrest from flow. *Am J Physiol Heart Circ Physiol.* 2005; 289:H1976–H1984. [PubMed: 15937099]
27. Weber KS, von Hundelshausen P, Clark-Lewis I, Weber PC, Weber C. Differential immobilization and hierarchical involvement of chemokines in monocyte arrest and transmigration on inflamed endothelium in shear flow. *Eur J Immunol.* 1999; 29:700–712. [PubMed: 10064088]
28. Moser B, Loetscher P. Lymphocyte traffic control by chemokines. *Nat Immunol.* 2001; 2:123–128. [PubMed: 11175804]
29. Gerard C, Rollins BJ. Chemokines and disease. *Nat Immunol.* 2001; 2:108–115. [PubMed: 11175802]
30. Haskell CA, Cleary MD, Charo IF. Molecular uncoupling of fractalkine-mediated cell adhesion and signal transduction. Rapid flow arrest of CX3CR1-expressing cells is independent of G-protein activation. *J Biol Chem.* 1999; 274:10053–10058. [PubMed: 10187784]
31. Lauro C, Catalano M, Trettel F, Mainiero F, Ciotti MT, Eusebi F, Limatola C. The chemokine CX3CL1 reduces migration and increases adhesion of neurons with mechanisms dependent on the $\beta 1$ integrin subunit. *J Immunol.* 2006; 177:7599–7606. [PubMed: 17114429]
32. Kerfoot SM, Lord SE, Bell RB, Gill V, Robbins SM, Kubes P. Human fractalkine mediates leukocyte adhesion but not capture under physiological shear conditions; a mechanism for selective monocyte recruitment. *Eur J Immunol.* 2003; 33:729–739. [PubMed: 12616493]
33. Takagi J, Erickson HP, Springer TA. C-terminal opening mimics 'inside-out' activation of integrin $\alpha 5 \beta 1$. *Nat Struct Biol.* 2001; 8:412–416. [PubMed: 11323715]
34. Tam SH, Sassoli PM, Jordan RE, Nakada MT. Abciximab (ReoPro, chimeric 7E3 Fab) demonstrates equivalent affinity and functional blockade of glycoprotein IIb/IIIa and $\alpha (v) \beta 3$ integrins. *Circulation.* 1998; 98:1085–1091. [PubMed: 9736595]
35. Hall DE, Reichardt LF, Crowley E, Holley B, Moezzi H, Sonnenberg A, Damsky CH. The $\alpha 1 \beta 1$ and $\alpha 6 \beta 1$ integrin heterodimers mediate cell attachment to distinct sites on laminin. *J Cell Biol.* 1990; 110:2175–2184. [PubMed: 2351695]
36. Takada Y, Puzon W. Identification of a regulatory region of integrin $\alpha 1$ subunit using activating and inhibiting antibodies. *J Biol Chem.* 1993; 268:17597–17601. [PubMed: 7688727]
37. Irie A, Kamata T, Puzon-McLaughlin W, Takada Y. Critical amino acid residues for ligand binding are clustered in a predicted β -turn of the third N-terminal repeat in the integrin $\alpha 4$ and $\alpha 5$ subunits. *Embo J.* 1995; 14:5550–5556. [PubMed: 8521812]
38. Blystone SD, Graham IL, Lindberg FP, Brown EJ. Integrin $\alpha v \beta 3$ differentially regulates adhesive and phagocytic functions of the fibronectin receptor $\alpha 5 \beta 1$. *J Cell Biol.* 1994; 127:1129–1137. [PubMed: 7525603]
39. Saegusa J, Akakura N, Wu CY, Hoogland C, Ma Z, Lam KS, Liu FT, Takada YK, Takada Y. Pro-inflammatory secretory phospholipase A2 type IIA binds to integrins $\alpha v \beta 3$ and $\alpha 4 \beta 1$ and induces proliferation of monocytic cells in an integrin-dependent manner. *J Biol Chem.* 2008; 283:26107–26115. [PubMed: 18635536]
40. Saegusa J, Yamaji S, Ieguchi K, Wu CY, Lam KS, Liu FT, Takada YK, Takada Y. The direct binding of insulin-like growth factor-1 (IGF-1) to integrin $\alpha v \beta 3$ is involved in IGF-1 signaling. *J Biol Chem.* 2009; 284:24106–24114. [PubMed: 19578119]

41. Mori S, Wu CY, Yamaji S, Saegusa J, Shi B, Ma Z, Kuwabara Y, Lam KS, Isseroff RR, Takada YK, Takada Y. Direct Binding of Integrin $\alpha\text{v}\beta\text{3}$ to FGF1 Plays a Role in FGF1 Signaling. *J Biol Chem.* 2008; 283:18066–18075. [PubMed: 18441324]
42. Mizoue LS, Sullivan SK, King DS, Kledal TN, Schwartz TW, Bacon KB, Handel TM. Molecular determinants of receptor binding and signaling by the CX3C chemokine fractalkine. *J Biol Chem.* 2001; 276:33906–33914. [PubMed: 11432858]
43. Harrison JK, Fong AM, Swain PA, Chen S, Yu YR, Salafranca MN, Greenleaf WB, Imai T, Patel DD. Mutational analysis of the fractalkine chemokine domain. Basic amino acid residues differentially contribute to CX3CR1 binding, signaling, and cell adhesion. *J Biol Chem.* 2001; 276:21632–21641. [PubMed: 11278650]
44. Aumailley M, Gurrath M, Muller G, Calvete J, Timpl R, Kessler H. Arg-Gly-Asp constrained within cyclic pentapeptides. Strong and selective inhibitors of cell adhesion to vitronectin and laminin fragment P1. *FEBS Lett.* 1991; 291:50–54. [PubMed: 1718779]
45. Takagi J, Kamata T, Meredith J, Puzon-McLaughlin W, Takada Y. Changing ligand specificities of $\alpha\text{v}\beta\text{1}$ and $\alpha\text{v}\beta\text{3}$ integrins by swapping a short diverse sequence of the β subunit. *J Biol Chem.* 1997; 272:19794–19800. [PubMed: 9242639]
46. Xiong JP, Stehle T, Zhang R, Joachimiak A, Frech M, Goodman SL, Arnaout MA. Crystal structure of the extracellular segment of integrin $\alpha\text{v}\beta\text{3}$ in complex with an Arg-Gly-Asp ligand. *Science.* 2002; 296:151–155. [PubMed: 11884718]
47. Triantafilou M, Triantafilou K, Wilson KM, Takada Y, Fernandez N. High affinity interactions of Coxsackievirus A9 with integrin $\alpha\text{v}\beta\text{3}$ (CD51/61) require the CYDMKTTTC sequence of β3 , but do not require the RGD sequence of the CAV-9 VP1 protein. *Hum Immunol.* 2000; 61:453–459. [PubMed: 10773347]
48. Yokoyama K, Zhang XP, Medved L, Takada Y. Specific binding of integrin $\alpha\text{v}\beta\text{3}$ to the fibrinogen gamma and αE chain C-terminal domains. *Biochemistry.* 1999; 38:5872–5877. [PubMed: 10231539]
49. Ieguchi K, Fujita M, Ma Z, Davari P, Taniguchi Y, Sekiguchi K, Wang B, Takada YK, Takada Y. Direct binding of the EGF-like domain of neuregulin-1 to integrins ($\alpha\text{v}\beta\text{3}$ and $\alpha\text{6}\beta\text{4}$) is involved in neuregulin-1/ErbB signaling. *J Biol Chem.* 2010; 285:31388–31398. [PubMed: 20682778]
50. Harrison JK, Jiang Y, Chen S, Xia Y, Maciejewski D, McNamara RK, Streit WJ, Salafranca MN, Adhikari S, Thompson DA, Botti P, Bacon KB, Feng L. Role for neuronally derived fractalkine in mediating interactions between neurons and CX3CR1-expressing microglia. *Proc Natl Acad Sci U S A.* 1998; 95:10896–10901. [PubMed: 9724801]
51. Ruoslahti E. Integrins. *J Clin Invest.* 1991; 87:1–5. [PubMed: 1985087]
52. Humphries MJ. The molecular basis and specificity of integrin-ligand interactions. *J Cell Sci.* 1990; 97(Pt 4):585–592. [PubMed: 2077034]
53. Mould AP, Askari JA, Craig SE, Garratt AN, Clements J, Humphries MJ. Integrin $\alpha\text{4}\beta\text{1}$ -mediated melanoma cell adhesion and migration on vascular cell adhesion molecule-1 (VCAM-1) and the alternatively spliced IIICS region of fibronectin. *J Biol Chem.* 1994; 269:27224–27230. [PubMed: 7525548]
54. Peled A, Grabovsky V, Habler L, Sandbank J, Arenzana-Seisdedos F, Petit I, Ben-Hur H, Lapidot T, Alon R. The chemokine SDF-1 stimulates integrin-mediated arrest of CD34(+) cells on vascular endothelium under shear flow. *J Clin Invest.* 1999; 104:1199–1211. [PubMed: 10545519]
55. Peled A, Kollet O, Ponomaryov T, Petit I, Franitza S, Grabovsky V, Slav MM, Nagler A, Lider O, Alon R, Zipori D, Lapidot T. The chemokine SDF-1 activates the integrins LFA-1, VLA-4, and VLA-5 on immature human CD34(+) cells: role in transendothelial/stromal migration and engraftment of NOD/SCID mice. *Blood.* 2000; 95:3289–3296. [PubMed: 10828007]
56. Sanz-Rodriguez F, Hidalgo A, Teixido J. Chemokine stromal cell-derived factor-1 α modulates VLA-4 integrin-mediated multiple myeloma cell adhesion to CS-1/fibronectin and VCAM-1. *Blood.* 2001; 97:346–351. [PubMed: 11154207]
57. Potter PK, Cortes-Hernandez J, Quartier P, Botto M, Walport MJ. Lupus-prone mice have an abnormal response to thioglycolate and an impaired clearance of apoptotic cells. *J Immunol.* 2003; 170:3223–3232. [PubMed: 12626581]

58. Puzon-McLaughlin W, Kamata T, Takada Y. Multiple discontinuous ligand-mimetic antibody binding sites define a ligand binding pocket in integrin $\alpha(\text{IIb})\beta(3)$. *J Biol Chem*. 2000; 275:7795–7802. [PubMed: 10713093]
59. Artoni A, Li J, Mitchell B, Ruan J, Takagi J, Springer TA, French DL, Collier BS. Integrin $\beta(3)$ regions controlling binding of murine mAb 7E3: implications for the mechanism of integrin $\alpha(\text{IIb})\beta(3)$ activation. *Proc Natl Acad Sci U S A*. 2004; 101:13114–13120. [PubMed: 15277669]
60. Kawaguchi M, Hosotani R, Ohishi S, Fujii N, Tulachan SS, Koizumi M, Toyoda E, Masui T, Nakajima S, Tsuji S, Ida J, Fujimoto K, Wada M, Doi R, Imamura M. A novel synthetic Arg-Gly-Asp-containing peptide cyclo(-RGDf==V-) is the potent inhibitor of angiogenesis. *Biochem Biophys Res Commun*. 2001; 288:711–717. [PubMed: 11676501]
61. Nanki T, Urasaki Y, Imai T, Nishimura M, Muramoto K, Kubota T, Miyasaka N. Inhibition of fractalkine ameliorates murine collagen-induced arthritis. *J Immunol*. 2004; 173:7010–7016. [PubMed: 15557198]
62. Suzuki F, Nanki T, Imai T, Kikuchi H, Hirohata S, Kohsaka H, Miyasaka N. Inhibition of CX3CL1 (fractalkine) improves experimental autoimmune myositis in SJL/J mice. *J Immunol*. 2005; 175:6987–6996. [PubMed: 16272359]

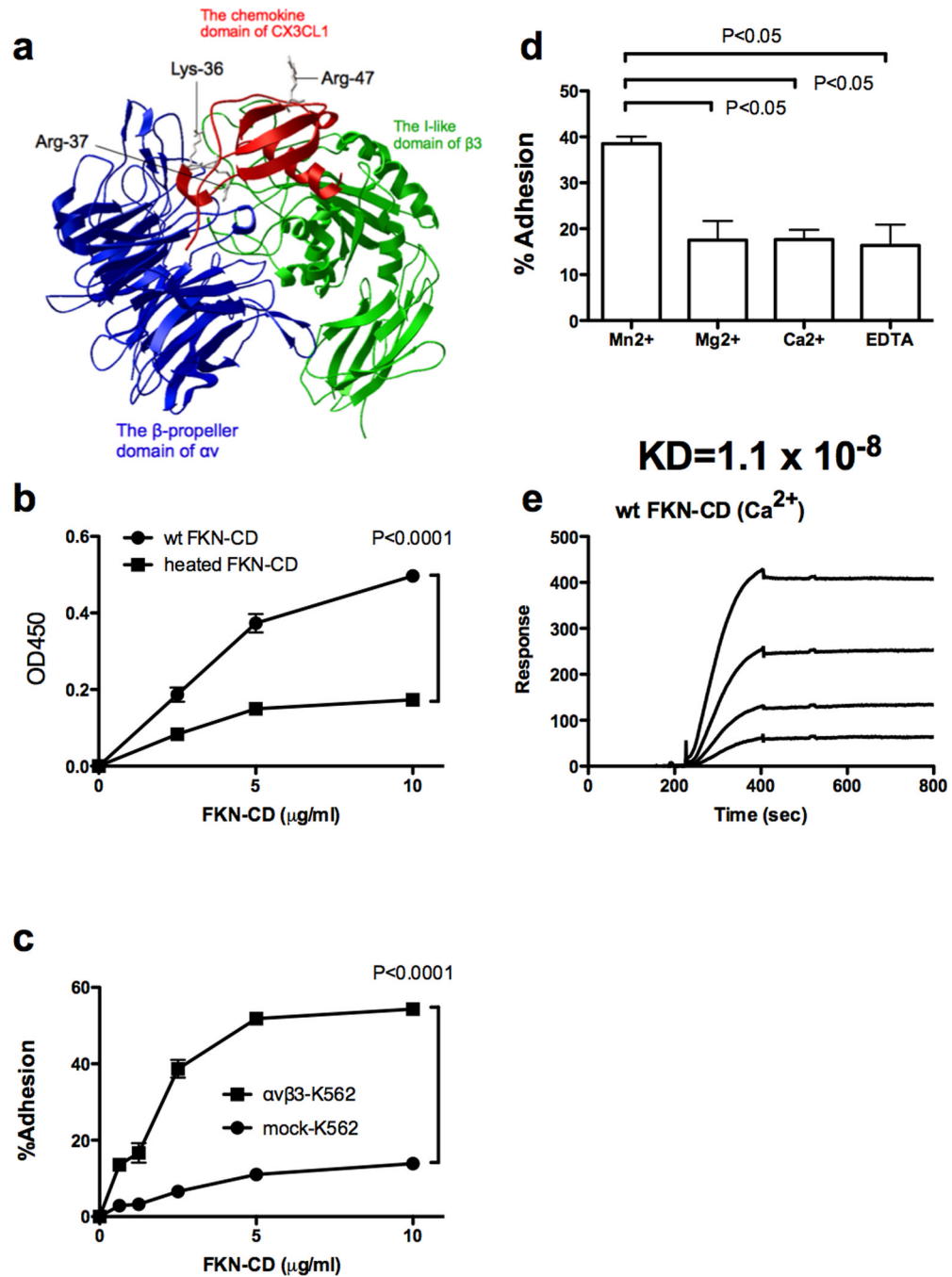


Fig. 1. $\alpha v\beta 3$ binds to FKN-CD

a) A model of FKN-CD-integrin $\alpha v\beta 3$ interaction predicted by docking simulation using AutoDock3. The headpiece of integrin $\alpha v\beta 3$ (PDB code 1LG5) was used as a target. The model predicts that the FKN-CD (PDB code 1F2L, red) binds to the RGD-binding site of the integrin $\alpha v\beta 3$ headpiece (blue and green). The Lys36, and Arg37 of FKN-CD are located at the interface between FKN-CD and $\alpha v\beta 3$, and selected for mutagenesis studies. Arg47 that is involved in CX3CR1 binding is not located in the predicted integrin-binding site. b) Binding of FKN-CD to soluble $\alpha v\beta 3$. FKN-CD binding to recombinant soluble $\alpha v\beta 3$ was measured in ELISA-type assays. Wells of 96-well microtiter plates were coated with FKN-CD, and the remaining protein-binding sites were blocked with BSA. Soluble recombinant

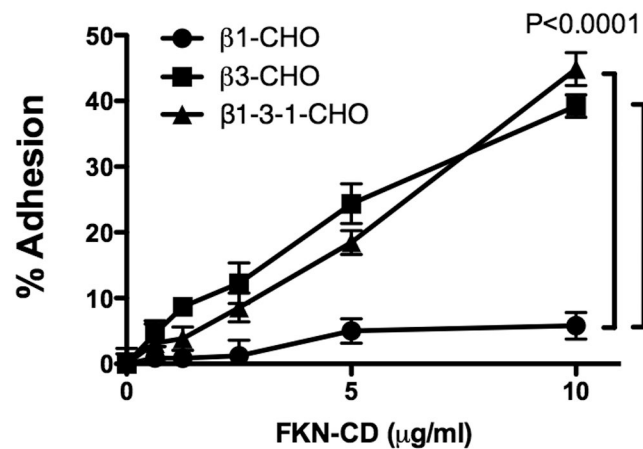
integrin $\alpha v\beta 3$ (5 $\mu\text{g}/\text{ml}$) was added to the wells in the presence of 1 mM Mn^{2+} and incubated for 2 h at room temperature. Bound $\alpha v\beta 3$ was determined using anti- $\beta 3$ antibody and HRP-conjugated anti-mouse IgG. Data are shown as means \pm S.E. of three independent experiments. c) Adhesion of K562 cells that express integrin $\alpha v\beta 3$ to FKN-CD. Wells of 96-well microtiter plates were coated with FKN-CD, and the remaining protein-binding sites were blocked with BSA. Cells were added to the wells and incubated for 1 h at 37 °C in RPMI1640, and bound cells were quantified by using phosphatase assays. Data are shown as means \pm S.E. of three independent experiments. d) Cation dependency of FKN-CD- $\alpha v\beta 3$ interaction. Adhesion assays of $\alpha v\beta 3$ -K562 cells to FKN-CD were performed as described in Fig. 1c in Tyrode-HEPES containing 4 mM cations. FKN-CD was used at the 2.5 $\mu\text{g}/\text{ml}$ coating concentration. Data are shown as means \pm S.E. of three independent experiments.

e) Surface plasmon resonance (SPR) study of integrin $\alpha v\beta 3$ -FKN-CD interaction. Binding of FKN-CD to $\alpha v\beta 3$ in SPR. Soluble $\alpha v\beta 3$ was immobilized on a CM5 sensor chip. wt FKN-CD was individually 2-fold serially diluted from 1.1 μM to 138 nM in HBS-P buffer with 1 mM of Ca^{2+} .

a

$\beta 1$	S-TTPAKLRN	ECTS-EQNCITTPFSY
$\beta 3$	YISPPEALEN	EICYDMKTTCLPMFGY
$\beta 1-3-1$	S-TTPAKLRN	EICYDMKTTCTTPFSY

b



c

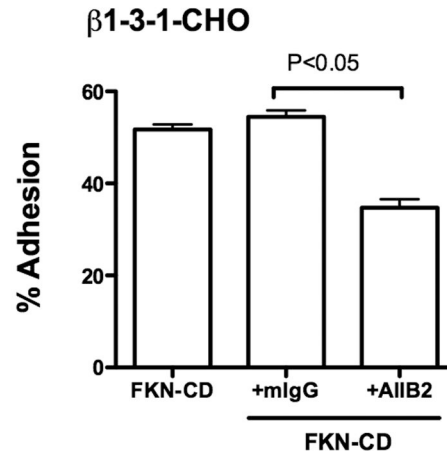


Fig. 2. The $\beta 3$ specificity loop is involved in FKN-CD binding to $\alpha v\beta 3$

a) Alignment of $\beta 1$, $\beta 1-3-1$, and $\beta 3$ sequences around the specificity loop region (in the boxed area). The specificity loop is located in the ligand-binding site of $\beta 3$ and is exposed to the surface. The $\beta 1-3-1$ mutation, in which the $\beta 1$ sequence in the specificity loop is changed to the corresponding $\beta 3$ sequence, changes the specificity of $\beta 1$ integrins to that of $\beta 3$ integrins (see text for details). b). Adhesion of CHO cells that express human $\beta 3$ ($\beta 3$ -CHO), $\beta 1$ ($\beta 1$ -CHO) or $\beta 1-3-1$ ($\beta 1-3-1$ -CHO) to FKN-CD. Adhesion assays were performed as described in Fig. 1 except that DMEM was used. Data are shown as means \pm S.E. of three independent experiments. c) $\beta 1-3-1$ -CHO cells adhesion to FKN-CD was blocked by anti-human $\beta 1$ antibody AIIB2 (10 $\mu\text{g/ml}$), but not by purified mouse IgG

(mIgG). FKN-CD was used at 5 $\mu\text{g}/\text{ml}$. Adhesion assays were performed as described in Fig. 1 except that DMEM was used. Data are shown as means \pm S.E. of three independent experiments.

\$watermark-text

\$watermark-text

\$watermark-text

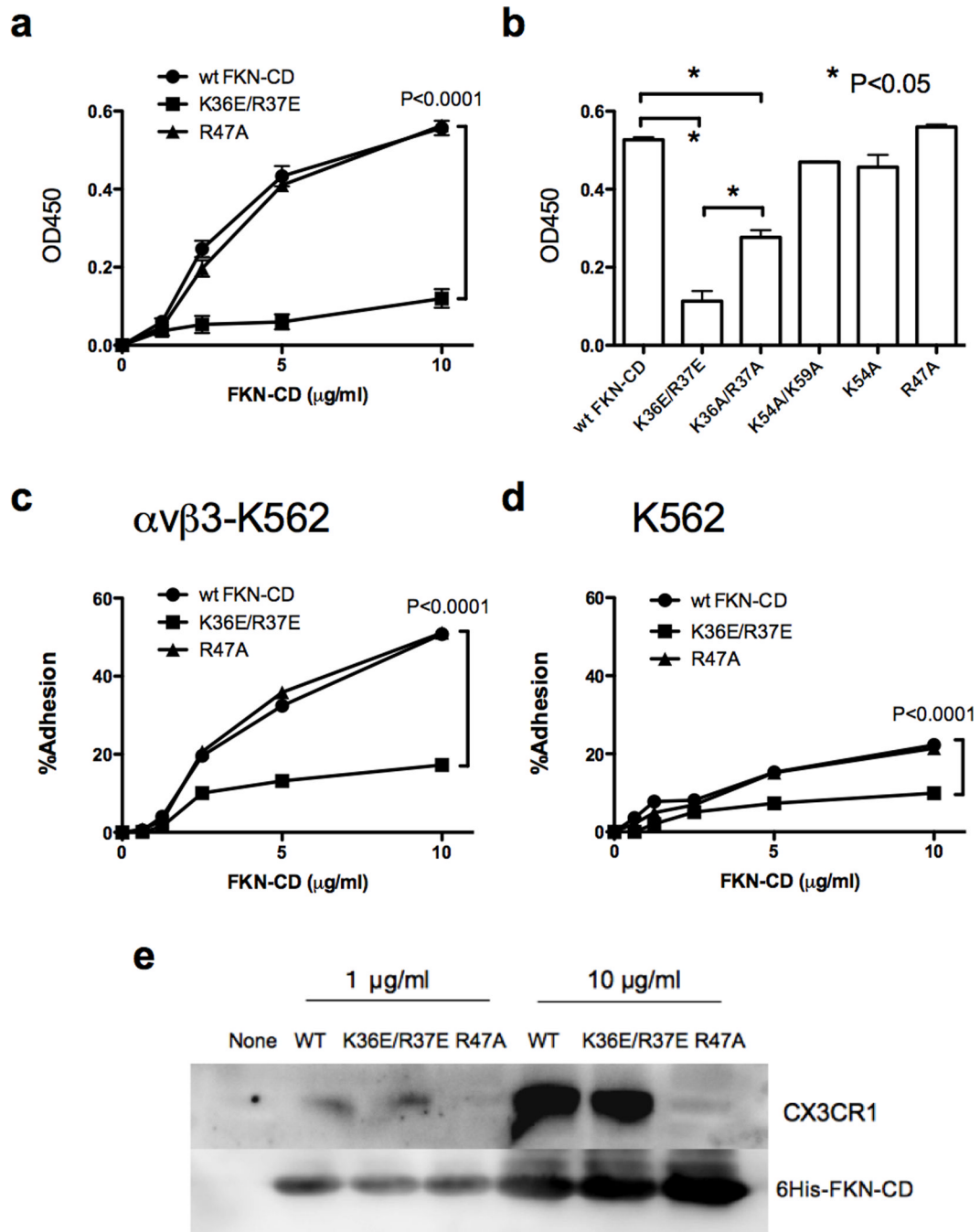


Fig. 3. An integrin-binding defective mutant of FKN-CD

a) The K36E/R37E FKN-CD mutant was defective in binding to $\alpha\text{v}\beta\text{3}$. FKN-CD binding to recombinant soluble $\alpha\text{v}\beta\text{3}$ was measured in ELISA-type assays as described in Fig. 1. Data are shown as means \pm S.E. of three independent experiments. b) Summary of the effect of mutations in the predicted integrin-binding site in FKN-CD. Several different FKN-CD mutants were immobilized to wells of 96-well microtiter plates (10 $\mu\text{g/ml}$) and the binding of soluble $\alpha\text{v}\beta\text{3}$ was measured in the presence of 1 mM Mn^{2+} as described in Fig. 1. Data are shown as means \pm S.E. of three independent experiments. c and d) The effect of the K36E/R37E mutation on the adhesion of $\alpha\text{v}\beta\text{3-K562}$ or K562 cells to FKN-CD. Adhesion assays were performed as described in Fig. 1. Data are shown as means \pm S.E. of three

independent experiments. e) K36E/R37E binds to CX3CR1 at a level comparable with wt FKN. U937 cell lysates were treated with 1 or 10 $\mu\text{g/ml}$ FKN-CD (wt or mutant) in RPMI1640 for 15 min at 37°C. FKN-CD (6His-tagged) was purified from cell lysates using Ni-NTA beads and purified materials were analyzed by Western blotting.

\$watermark-text

\$watermark-text

\$watermark-text

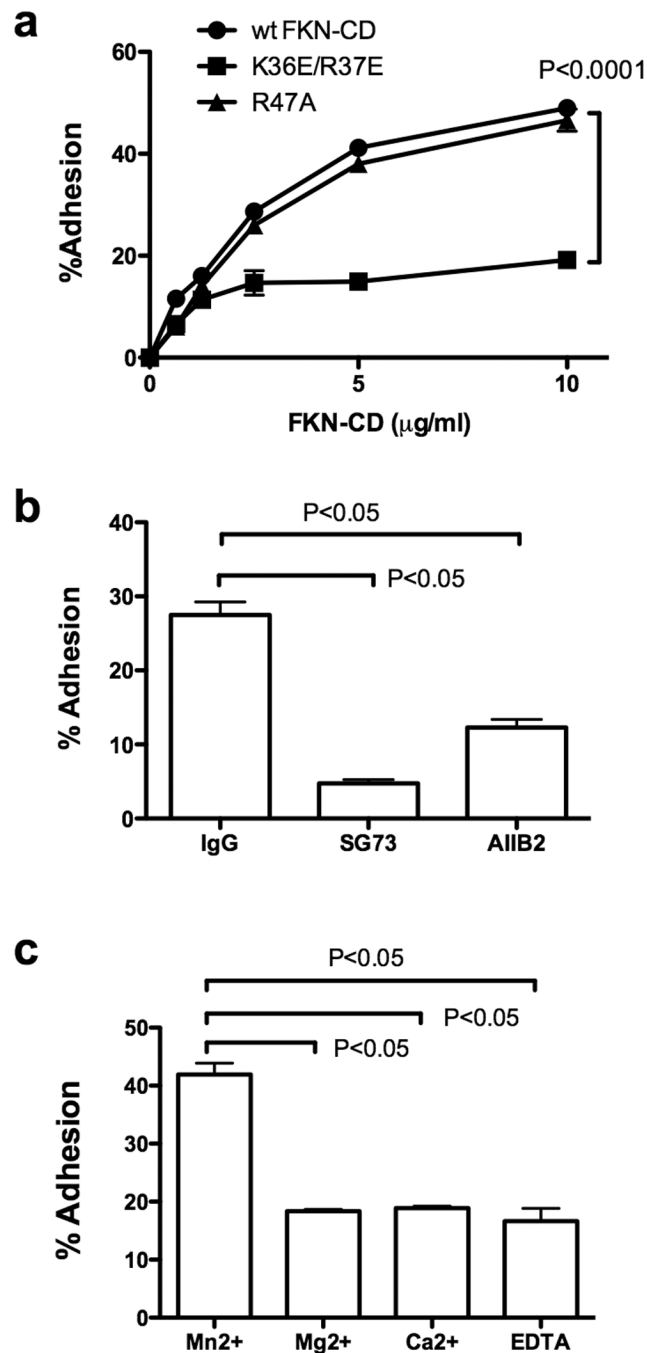


Fig. 4. Integrin $\alpha 4\beta 1$ binds to FKN-CD

a) Adhesion of K562 cells that express recombinant human $\alpha 4$ ($\alpha 4$ -K562 cells). Adhesion assays were performed as described in Fig. 1. Data are shown as means \pm S.E. of three independent experiments. b) Effect of antagonists to integrins on adhesion of $\alpha 4$ -K562 cells to FKN-CD. Adhesion assays were performed as described in Fig. 1. FKN-CD was used at the 2.5 $\mu\text{g/ml}$ coating concentration. mIgG (20 $\mu\text{g/ml}$), SG73 (anti-human $\alpha 4$, 10 $\mu\text{g/ml}$) and AIB2 (anti-human $\beta 1$, 20 $\mu\text{g/ml}$) were used at the indicated final concentrations. Data are shown as means \pm S.E. of three independent experiments. c) Cation requirement of $\alpha 4\beta 1$ -FKN-CD interaction. Adhesion assays were performed as described in Fig. 1 in Tyrode-

HEPES containing 4 mM cations. Data are shown as means \pm S.E. of three independent experiments.

\$watermark-text

\$watermark-text

\$watermark-text

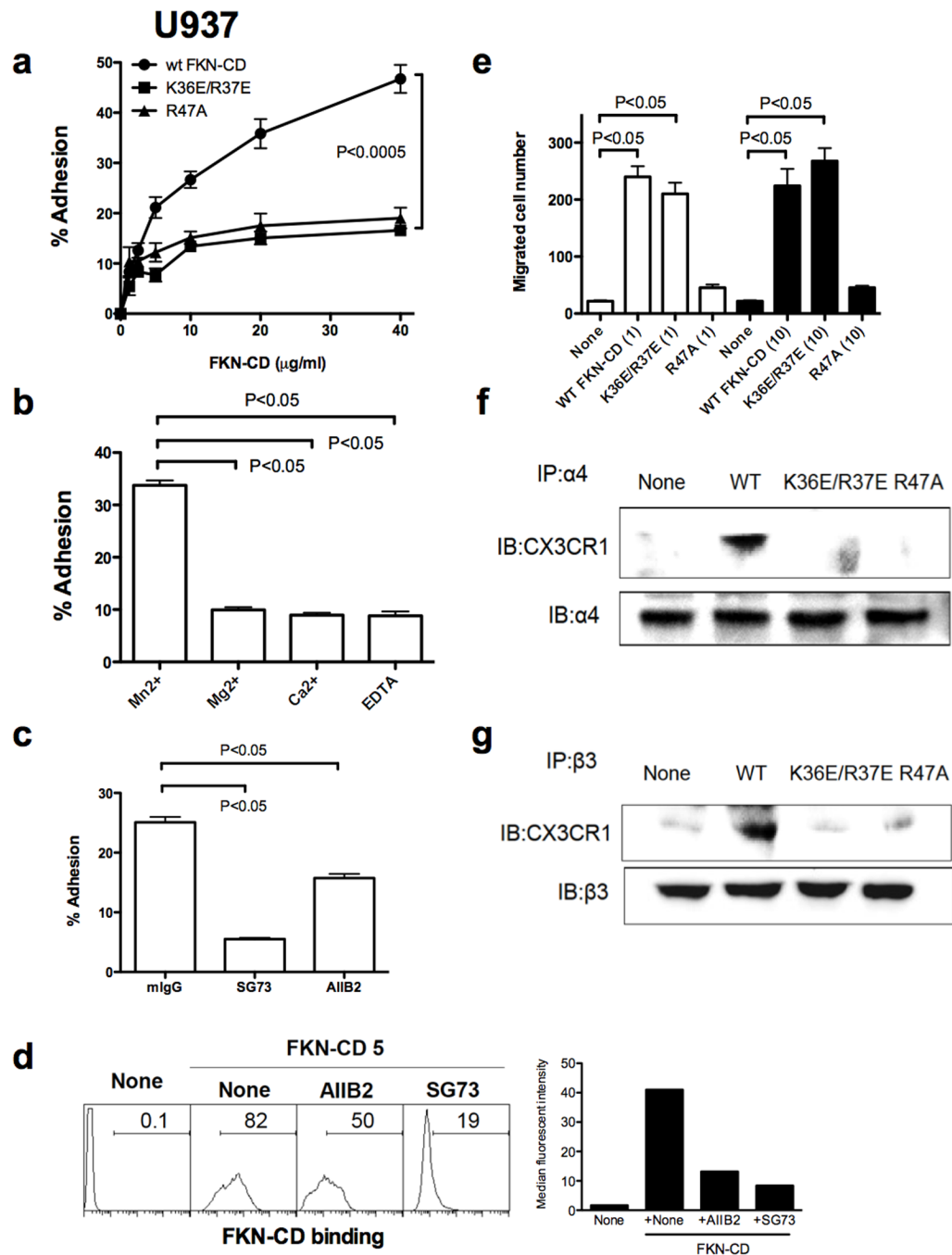


Fig. 5. U937 monocytic cells bind to FKN-CD

a) Adhesion of U937 cells (CX3CR1+) to FKN-CD. Adhesion assays were performed in RPMI1640 as described in Fig. 1. Data are shown as means \pm S.E. of three independent experiments. The data suggest that integrins and CX3CR1 contribute to U937 adhesion to FKN-CD. b) Cation requirement of adhesion of U937 cells to FKN-CD. Adhesion assays were performed as described in Fig. 1 in Tyrode-HEPES containing 4 mM cations. FKN-CD was used at the 2.5 μ g/ml coating concentration. Data are shown as means \pm S.E. of three independent experiments. c) Effect of anti- α 4 antibody on adhesion of U937 cells to FKN-CD. Adhesion assays in RPMI1640 were performed as described in Fig. 1. FKN-CD (20 μ g/ml) was used for coating. Cells were pre-incubated with SG73 (10 μ g/ml) or AIIB2 (20 μ g/ml).

ml) before adhesion assays. Data are shown as means \pm S.E. of three independent experiments. The data suggest that $\alpha 4\beta 1$ antagonists partially suppress U937 adhesion to FKN-CD. d) Inhibition of the binding of labeled FKN-CD to U937 cells. U937 cells were incubated with FITC-labeled FKN-CD (5 $\mu\text{g}/\text{ml}$) in the presence of mAb AIIB2 (anti- $\beta 1$, 20 $\mu\text{g}/\text{ml}$) or SG73 (anti- $\alpha 4$, 10 $\mu\text{g}/\text{ml}$), and the binding of FKN-CD was measured in flow cytometry. The number is %positive cells. The histograms shown are representatives of three experiments. e) wt FKN-CD and K36E/R37E induce chemotaxis of U937 cells at comparable levels, but R47A does not. Chemotaxis was measured in modified Boyden chambers (Transwells). wt FKN, R36E/R37E, or R47A (1 and 10 ng/ml, total 600 μl RPMI 1640 medium) was placed in the lower chamber, and U937 cells (5×10^5 cells per well) were placed in the upper chamber. After 4hr incubation at 37°C, cells in the lower chamber was counted. f) and g) FKN-CD induces co-precipitation of integrins and CX3CR1, while K36E/R37E does not. U937 cells were treated with 1 $\mu\text{g}/\text{ml}$ FKN-CD (wt or mutant) in RPMI1640 for 15 min at 37°C. Integrins were immunopurified from cell lysates using anti- $\alpha 4$ (f) or anti- $\beta 3$ (g), and immunopurified materials were analyzed by Western blotting.

\$watermark-text

\$watermark-text

\$watermark-text

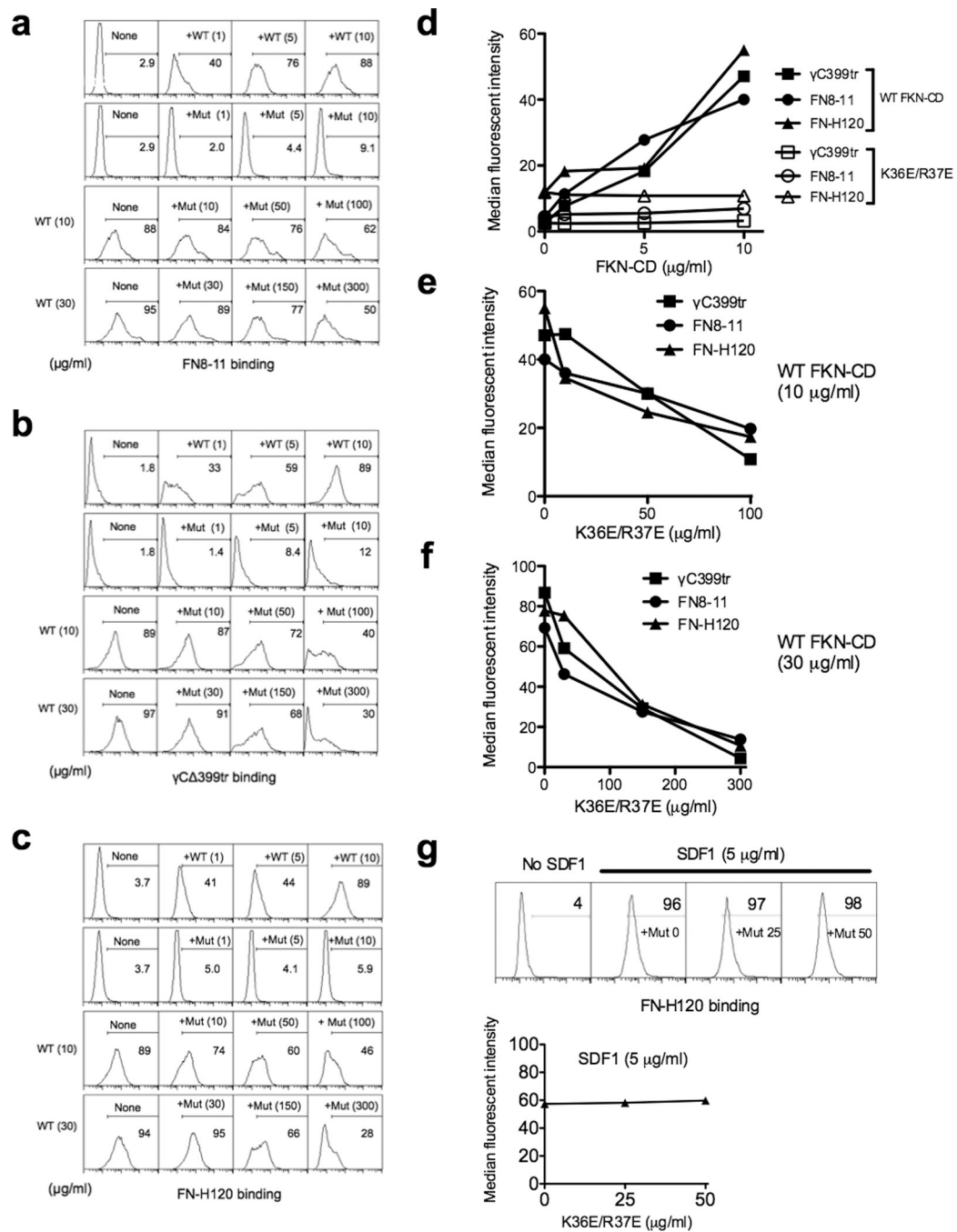


Fig. 6. Dominant-negative effect of K36E/R37E on integrin ligand interaction

a–c. Binding of FITC-labeled ligands to U937 cells was measured in flow cytometer. Ligands used are a) fibronectin domains 8–11 (FN8–11), a specific ligand to $\alpha 5\beta 1$; b) fibrinogen γ -chain C-terminal domain that lacks residues 400–411 ($\gamma\text{C}\Delta 399\text{tr}$), a specific ligand for $\alpha \nu\beta 3$, and c) fibronectin H120 fragment (FN-H120), a specific ligand to $\alpha 4\beta 1$. Cells were incubated with the ligands (10 $\mu\text{g/ml}$) in the presence of wt FKN-CD and/or K36E/R37E (Mut) (the numbers in parentheses are concentrations in $\mu\text{g/ml}$). Data are shown as % positive cells. The histogram shown is a representative of three experiments. d), e), and f) Dose-dependent effect of FKN-CD on ligand binding to integrins. Median fluorescent intensity of ligand binding in a–c) was plotted against the concentrations of FKN-CD (wt

and K36E/R37E). g) Effect of K36E/R37E on SDF1-induced integrin activation. Binding of FITC-labeled ligands to U937 cells was measured in flow cytometer. Cells were incubated with FITC-labeled fibronectin H120 fragment (FN-H120), a specific ligand to $\alpha 4\beta 1$, (10 $\mu\text{g}/\text{ml}$) in the presence of SDF1 (5 $\mu\text{g}/\text{ml}$) and K36E/R37E (Mut) (the numbers are concentrations in $\mu\text{g}/\text{ml}$). Data are shown as % positive cells. The histogram shown is a representative of three experiments. Median fluorescent intensity was plotted against the concentration of K36E/R37E (bottom).

\$watermark-text

\$watermark-text

\$watermark-text

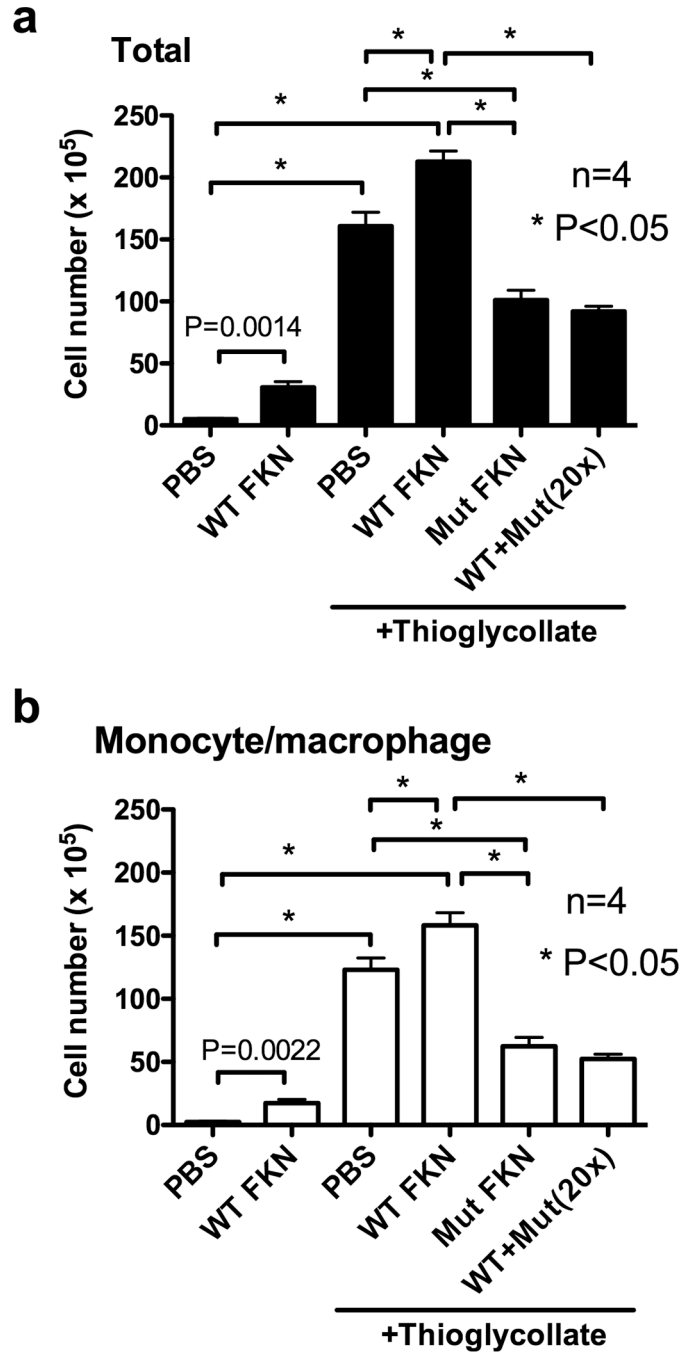


Fig. 7. Anti-inflammatory effect of K36E/R37E in thioglycollate-induced peritonitis
 a) Total cell number and b) monocyte/macrophage. We injected K36E/R37E (100 µg) or the mixture of wt FKN-CD (100 µg) and excess (2000 µg) K36E/R37E to mice and 3 h later injected i.p. 1 ml 3% thioglycollate. Mice were killed 48 h after thioglycollate injection, and peritoneal exudate cells were harvested by peritoneal lavage using ice-cold RPMI1640/10% FBS. Cells were counted on a hemocytometer and then differential cell counts were conducted after staining with Hem-3 (Fischer). Data are shown as means ± S.E. Statistical analysis was performed using one-way ANOVA and Tukey post-hoc analysis, except that t-test was used for PBS and WT FKN. Approx. 70% of the exudate cells was macrophages/monocytes 48 h after thioglycollate injection, which is consistent with previous reports (57).

The data suggest that K36E/R37E has an anti-inflammatory effect, and neutralizes endogenous and exogenous FKN (the dominant-negative effect).

\$watermark-text

\$watermark-text

\$watermark-text

Table 1

Amino acid residues predicted to be involved in FKN-CD- α v β 3 interaction. Amino acid residues in integrin α v β 3 and FKN-CD within 6 Å to each other in the docking model were identified using Swiss-pdb viewer.

FKN-CD	Integrin α v	Integrin β 3
Thr6, Lys18, Val21, Tyr27, Gln29, Asn30, Gln31, Ala32, Ser33, Gly35, Lys36, Arg37, Ala38, Ileu39, Asp52, Pro53, Lys54, Glu55, Gln56, Trp57, Val58, Lys59, Asp60, Met62, Gln63, His64, Asp66, Arg67	Asp146, Ileu147, Asp148, Ala149, Asp150, Gly151, Phe177, Tyr178, Try179, Gln180, Arg211, Thr212, Ala213, Gln214, Ala215, Ile216, Asp218	Ser121, Tyr122, Ser123, Met124, Lys125, Asp126, Asp127, Tyr166, Cys177, Asp179, Met180, Thr182, Arg214, Asn215, Arg216, Asp217, Ala218, Thr311, Glu312, Asn313, Val314, Leu333, Ser334, Met335, Asp336, Ser337